

TWO-PION INTERFEROMETRY FOR GRANULAR SOURCES

Wei-Ning Zhang

School of Physics and Optoelectronic Technology, Dalian University of Technology, Dalian, China

A review on the two-pion Hanbury–Brown–Twiss (HBT) interferometry in the granular source model of quark–gluon plasma droplets is presented. The characteristic quantities of the granular source extracted by imaging analysis are presented and compared with the HBT radii obtained by the usual Gaussian formula fit. The signals of granular sources are presented.

PACS: 25.75.-q

INTRODUCTION

The main purpose of relativistic heavy-ion collisions is the study of the quark–gluon plasma (QGP) formed in the early stage of the collisions. As is well known, the system produced in the collisions may thermalize and reach local equilibrium in a very short time τ_0 . The following evolution can be described by hydrodynamics. Hydrodynamics provides a direct link between the early state and final observables. It has been extensively used in relativistic heavy-ion collisions. However, the usual hydrodynamic calculations cannot explain the RHIC HBT data, $R_{\text{out}}/R_{\text{side}} \approx 1$, the so-called RHIC HBT puzzle [1].

In reference [2] a granular source model of QGP droplets was put forth for the HBT puzzle. In references [3,4] the granular source model was improved to explain the RHIC HBT data [1]. In reference [5], the fluctuations of the single-event two-pion correlation functions of granular sources were discussed. In references [6,7], some observables for granular sources were put forth and analyzed for the source inhomogeneity in the heavy-ion collisions at RHIC and Large Hadron Collider (LHC) energies. The imaging characteristic quantities and signals of the granular source of QGP droplets were presented in references [4,8]. This paper will give a review on the important ingredients and recent progresses of the granular source interferometry.

1. GRANULAR SOURCE MODEL OF QGP DROPLETS

The granular structure of QGP droplets may occur in the first-order phase transition from the QGP to hadronic gas, which was proposed by E. Witten in 1984 [9]. In [10,11], the two- and multi-pion HBT correlation functions of granular sources were investigated.

In two-pion interferometry, there is the relation among the HBT radii R_{out} and R_{side} , the transverse velocity of pion pair v_T , and source lifetime τ , $R_{\text{out}}^2 \approx R_{\text{side}}^2 + v_T^2 \tau^2$ [12]. In reference [2], it was noticed that the lifetime τ for a uniform hydrodynamic evolving source

scales with the source initial size. A smaller (or larger) initial source radius has a smaller (or larger) R_{side} , and smaller (or larger) source lifetime τ . So, there is always $R_{\text{out}} > R_{\text{side}}$ for the uniform hydrodynamic sources. However, for a granular source with small QGP droplets distributed in a large region, the source HBT radius R_{out} is approximately equal to R_{side} . It is because that for the granular source the HBT radius R_{side} (proportional to the QGP droplets distribution) is much larger than the source lifetime τ (proportional to the droplet radius).

In relativistic heavy-ion collisions, the system initial transverse energy density is highly fluctuating on event-by-event basis. The large initial fluctuations together with the effects of violent expansion and surface tension may lead to formation of granular droplets [3, 13]. On the other hand, the bulk viscosity of the QGP may increase rapidly near the QCD transition, which also leads to formation of the QGP droplets [14].

It is assumed in the improved granular source model [4] that the system produced in central relativistic heavy-ion collisions fragments and forms the QGP droplets at a time t_0 after τ_0 . The droplets distribute initially within a short cylinder along the beam direction (z direction) with the probabilities

$$\frac{dP_{\perp}}{2\pi\rho_0 d\rho_0} \propto \left[1 - \exp\left(-\frac{\rho_0^2}{\Delta\mathcal{R}_{\perp}^2}\right) \right] \theta(\mathcal{R}_{\perp} - \rho_0), \quad (1)$$

$$\frac{dP_y}{dy_0} = \theta(y_m - |y_0|), \quad z_0 = t_0 \tanh y_0, \quad (2)$$

where ρ_0 and z_0 are the initial transverse and longitudinal coordinates of the droplet center, y_0 is the initial rapidity of the droplet, \mathcal{R}_{\perp} , $\Delta\mathcal{R}_{\perp}$, and y_m are the radius of the cylinder, the shell parameter of the initial distribution, and the central rapidity limitation. On the basis of the Bjorken picture [15], the velocity of the droplet is assumed as

$$v_{d\perp} = a_T \left(\frac{\rho_0}{\mathcal{R}_{\perp}} \right)^{b_T} \sqrt{1 - v_{dz}^2}, \quad v_{dz} = \frac{z_0}{t_0}, \quad (3)$$

where a_T and b_T are the magnitude and exponential power parameters.

The evolution of the system after the fragmentation is the superposition of all the evolutions of the individual droplets, each of them is described by relativistic hydrodynamics with a cross-over equation of state of the entropy density [16]. The initial radius r'_0 of the droplets in local frame is assumed having a Gaussian distribution with standard deviation a . To include the pions emitted directly at hadronization and decayed from resonances later, the pion freeze-out temperature is taken in a wide region with the probability

$$\frac{dP_f}{dT} \propto f_{\text{dir}} \exp\left[-\frac{T - T_h}{\Delta T_{\text{dir}}}\right] + (1 - f_{\text{dir}}) \exp\left[-\frac{(T - T_h)}{\Delta T_{\text{dec}}}\right], \quad (4)$$

where f_{dir} is a fraction parameter for the direct emission, T_h is the temperature of complete hadronization, ΔT_{dir} and ΔT_{dec} describe the widths of temperature for the direct and decayed pion emissions.

The selections for the model parameter values can refer to [4].

2. GRANULAR SOURCE IMAGING

The imaging technique introduced by Brown, Danielewicz, and Pratt [17] is a model-independent way to extract the two-pion source function $S(r)$, the probability for emitting a pion pair with spatial separation r in the pair center-of-mass system (PCMS), from the HBT correlation function.

Figure 1, *a*, *b*, and *c* show the source functions of the granular source in x (out), y (side), and z (long) directions. Here k_T is the transverse momentum of pion pair in the longitudinally comoving system (LCMS). One can see that the source functions in out and long directions have long tails. The reason is the source expansion which boosts the pion pair in out and long directions. The source function width in long direction is smaller for larger k_T because the average longitudinal momentum of the pairs is smaller for larger k_T .

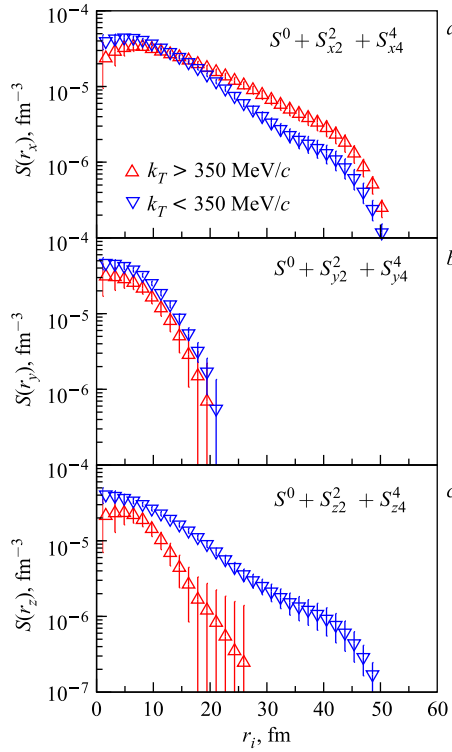


Fig. 1. Three-dimensional source functions of the granular source

Once the source functions are obtained, one can introduce the quantities of r moments to describe the source geometry numerically. They are model-independent quantities. Figure 2, *a-c* exhibits the quantities, $\tilde{R}_i = \sqrt{\pi}\langle r_i \rangle/2$, $i = x, y, z$, of the first-order moment $\langle r_i \rangle$ for the granular source. \tilde{R}_i describes the source size in i direction and normalized to the Gaussian radius for one-dimensional Gaussian source [4]. For comparing, the usual Gaussian fitted HBT radii of the granular source and RHIC experiments are shown in Fig. 2, *d-f*. In Fig. 2, *a*, the symbols ∇ denote the results of $\gamma_T^{-1}\tilde{R}_x$, where γ_T^{-1} is the Lorentz contracted

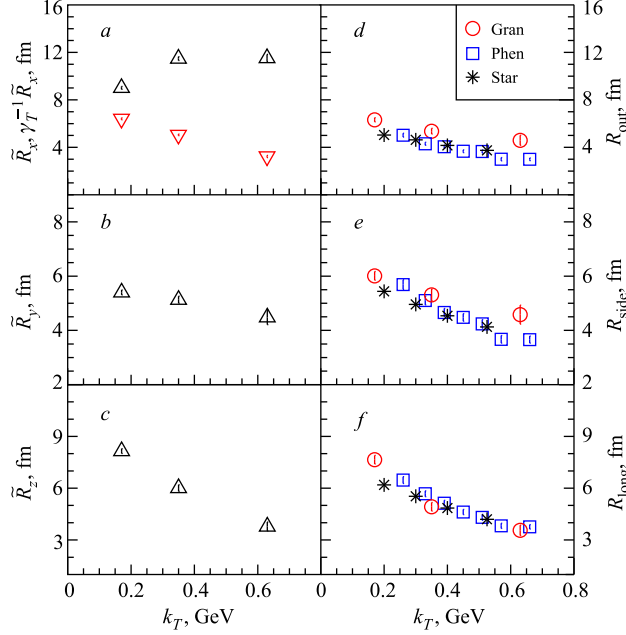


Fig. 2. *a-c*) Imaging results of granular source. *d-f*) HBT radii of granular source and RHIC experiments [1]

factor of LCMS to PCMS. One can see that the imaging results of \tilde{R}_i are consistent with the HBT radii after considering the Lorentz contraction.

3. GRANULAR SOURCE SIGNALS

For granular sources, the single-event HBT correlation functions exhibit large event-by-event fluctuations [5–7]. In order to observe the event-by-event fluctuations, we introduce the quantity f of the relative fluctuation of the single-event correlation function to mixed-event correlation function, with its error-inverses weight [6]

$$f(q_i) = \frac{|C_s(q_i) - C_m(q_i)|}{\Delta|C_s(q_i) - C_m(q_i)|}. \quad (5)$$

Figure 3 shows the distributions of the f for the variables of transverse relative momentum q_{trans} and relative momentum q of the pion pairs for the 40 events generated by the smoothed particle hydrodynamics [7, 18], with the impact parameter $b = 5$ fm. It can be seen that for the pion pair number $N_{\pi\pi} = 5 \cdot 10^6$, the distributions for the fluctuating initial conditions (FIC) are much wider than those for the smoothed initial conditions (SIC) for both q_{trans} and q . Even for $N_{\pi\pi} = 5 \cdot 10^5$, the widths for FIC are visibly larger than those for SIC. Figure 4 shows the root mean square (RMS) of f , as a function of $N_{\pi\pi}$ for the events. It can be seen that the values of f_{rms} rapidly increase with $N_{\pi\pi}$ for FIC because the errors in Eq. (5) decrease with $N_{\pi\pi}$. For SIC the values of f_{rms} are almost independent of $N_{\pi\pi}$, because both

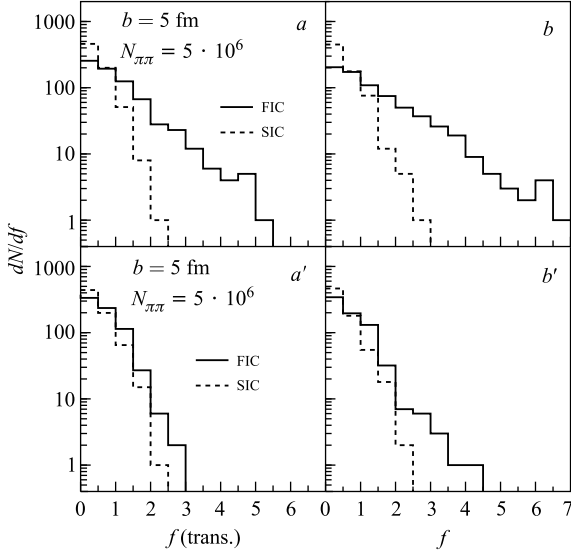


Fig. 3. The distributions dN/df for 40 events with FIC and SIC

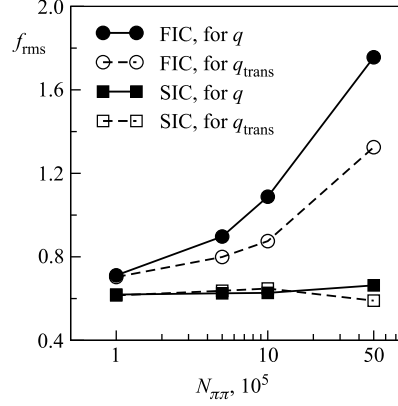


Fig. 4. The root mean square of f as a function of $N_{\pi\pi}$

the differences and their errors in Eq. (5) decrease with $N_{\pi\pi}$ in the case. At LHC energy the event multiplicity of identical pions is about two thousands and the order of $N_{\pi\pi}$ will be 10^6 . In this case, the distributions of f and its RMS will provide observable signals for the source inhomogeneity.

4. DISCUSSION AND CONCLUSION

In relativistic heavy-ion collisions, the fluctuating initial density distribution, violent expansion, surface tension, and viscosity of the QGP may lead to formation of the granular sources. For the granular sources, the single-event HBT correlation functions have large event-by-event fluctuations. Because of data statistics the experimental HBT analyses are performed with the mixed-event HBT correlation functions, and the fluctuations are smoothed out after the event average. However, the short lifetime of the granular source may survive and lead to the HBT puzzle. The model-independent quantities \bar{R}_i obtained by imaging analysis for the granular sources are consistent with the usual HBT radii of the granular sources and RHIC experiments. At the coming LHC heavy-ion collisions, it is hopefully to observe the signals of the granular sources.

REFERENCES

1. Adler C. *et al.* (STAR Collab.) // Phys. Rev. Lett. 2001. V. 87. P. 082301;
 Adcox K. *et al.* (PHENIX Collab.) // Phys. Rev. Lett. 2002. V. 88. P. 192302;
 Adler S. S. *et al.* (PHENIX Collab.) // Phys. Rev. Lett. 2004. V. 93. P. 152302;
 Adams J. *et al.* (STAR Collab.) // Phys. Rev. C. 2005. V. 71. P. 044906.

2. Zhang W. N., Efaaf M. J., Wong C. Y. // Phys. Rev. C. 2004. V. 70. P. 024903.
3. Zhang W. N., Ren Y. Y., Wong C. Y. // Phys. Rev. C. 2006. V. 74. P. 024908.
4. Zhang W. N., Yang Z. T., Ren Y. Y. // Phys. Rev. C. 2009. V. 80. P. 044908.
5. Wong C. Y., Zhang W. N. // Phys. Rev. C. 2004. V. 70. P. 064904.
6. Zhang W. N. *et al.* // Phys. Rev. C. 2005. V. 71. P. 064908.
7. Ren Y. Y., Zhang W. N., Liu J. L. // Phys. Lett. B. 2008. V. 669. P. 371.
8. Yang Z. T., Zhang W. N., Ren Y. Y. // J. Phys. G. 2009. V. 36. P. 015113.
9. Witten E. // Phys. Rev. D. 1984. V. 30. P. 272.
10. Pratt S., Siemens P. J., Vischer A. P. // Phys. Rev. Lett. 1992. V. 68. P. 1109.
11. Zhang W. N. *et al.* // Phys. Rev. C. 1995. V. 51. P. 922.
12. Wiedemann U. A., Heinz U. // Phys. Rep. 1999. V. 319. P. 145.
13. Zhang W. N., Wong C. Y. // Intern. J. Mod. Phys. E. 2007. V. 16. P. 3262;
Wong C. Y., Zhang W. N. // *Ibid.* P. 3271.
14. Torrieri G., Tomášik B., Mishustin I. // Phys. Rev. C. 2008. V. 77. P. 034903.
15. Bjorken J. D. // Phys. Rev. D. 1983. V. 27. P. 140.
16. Rischke D. H., Gyulassy M. // Nucl. Phys. A. 1996. V. 608. P. 479;
Blaizot J. P., Ollitrault J. Y. // Phys. Rev. D. 1987. V. 36. P. 916;
Laermann E. // Nucl. Phys. A. 1996. V. 610. P. 1.
17. Brown D. A., Danielewicz P. // Phys. Rev. C. 2001. V. 64. P. 014902;
Danielewicz P., Pratt S. // Phys. Rev. C. 2007. V. 75. P. 034907.
18. Aguiar C. E. *et al.* // J. Phys. G. 2001. V. 27. P. 75.